Article

A Kinematic Model to Compensate the Structural Deformations in Machine Tools Using Fibre Bragg Grating (FBG) Sensors

Francesco Aggogeri [1], Alberto Borboni [1], Rodolfo Faglia [1], Angelo Merlo [2] and Nicola Pellegrini [1,*]

[1] Department of Mechanical and Industrial Engineering, University of Brescia, via Branze, 38, 25123 Brescia, Italy; francesco.aggogeri@unibs.it (F.A.); alberto.borboni@unibs.it (A.B.); rodolfo.faglia@unibs.it (R.F.)

[2] CE.S.I Centro Studi Industriali, via Tintoretto, 10, 20093 Cologno Monzese, Italy; merlo@cesi.net

* Correspondence: nicola.pellegrini@unibs.it; Tel.: +39-0 30-371-5578

Abstract: Structural deformations are one of the most significant factor that affects machine tool (MT) positioning accuracy. These induced errors are complex to be represented by a model, nevertheless they need to be evaluated and predicted in order to increase the machining performance. This paper presents a novel approach to calibrate a machine tool in real-time, analyzing the thermo-mechanical errors through Fibre Bragg Grating (FBG) sensors embedded in the MT frame. The proposed configuration consists of an adaptronic structure of passive materials, Carbon Fibre Reinforced Polymers (CFRP), equipped by FBG sensors that are able to measure in real-time the deformed conditions of the frame. By using a proper thermo-mechanical kinematic model, the displacement of the end effector may be predicted and corrected when it is subjected to external undesired factors. By starting from a set of FE simulations to develop a model able to describe the MT structure stresses, a prototype has been fabricated and tested. The scope was to compare the numerical model with the experimental tests using FBG sensors. The experimental campaign has been performed varying the structure temperature over time and measuring the tool tip point (TTP) positions. The obtained results showed a substantial matching between the real and the predicted position of TTP confirming the effectiveness of the proposed calibration system.

Keywords: kinematic model; fiber Bragg grating; deformations; machine tools calibration; predicted model; multiple regression analysis; finite element analysis

1. Introduction

The positioning accuracy of a modern machine tool (MT) is one of the most important requirement to guarantee the machining precision and quality [1]. The accuracy of a MT related to the geometrical deviations may depend up to 60% on the stability of the structure and for the rest on workpiece fixturing and tools [2-4].

In the last years, researches have addressed their studies to mechatronic systems with the intention of compensating these undesired effects [5]. The principal causes of errors may be classified in geometrical errors and thermo-mechanical strains [6–10]. The first group is represented as the shape deviation that disturbs the moveable slides of the MT and may be assumed independent to the time. The second class is the result of external factors acting on the frame which are fundamentally time-correlated.

This work focuses on temperature oscillations that can origin three-dimensional thermal grades in MT structures and can produce non-linear distortions over time, impacting significantly on the machine accuracy [11,12].

The thermal distortions of the device components are generated by temperature gradients existing inside the structure. In order to model the temperature spreading and to compensate the consecutive distortion, it is important to get the temperature mapping in real-time, in particular when ultra-high precision machining is required. Although thermal errors might be reduced by

using structure materials with a low coefficient of thermal expansion, it is useful to consider a more reasonable method of decreasing thermal error such as an error compensation system. Recent studies have been carried out to introduce Polymeric Matrix Composites (PMC) fibers reinforced materials. Significant results related to mass reduction, stiffness increment and damping increase have been achieved. Nevertheless, the growing of customer requirements in terms of cutting machine performances has pushed the designers to investigate novel solutions. Calibration is a method where the existing thermal deviations are compensated correcting the position of the MT points in based on the magnitude of the thermal-mechanical error.

The state of art shows many works in the field of thermal-structural calibration [13]. Researchers have developed various procedures such as a simulation method [14, 16] in modelling the thermal characteristics. Obtaining a mathematical representation can be a complex process because it is problematic to produce the edge limitations and get the characteristic of heat transmission. The test of the machine tool is still required to calibrate the model for a successful application of the technique. Different model structures have been used to calculate thermal errors such as (MRA) Multiple Regression Analysis [17], (ANN) artificial neural networks [18], fuzzy logic [19], an adaptive neuro-fuzzy implication [20,21], and a grouping of diverse modelling procedures [22,23]. Early work by Chen et al. [15] used both a MRA model and an ANN model for thermal error compensation of a horizontal machining center. Thanks to their experimental results, it was possible to decrease the thermal error from 200 to 30 μm.

Wang [22] applied a Hierarchy-Genetic-Algorithm (HGA) trained neural network with the aim of mapping the temperature change against the thermal response of the MT. Experimental results pointed out that the temperature inaccuracy model could moderate the deviation to smaller than 10μm under real conditions. Nowadays, there is a number of different approaches to solve this problem [22], which can be grouped in two main categories: design-based techniques and compensation-based methods. The first category collects all those good practice design techniques that permit to develop a MT based on a structure that is stable, stiff, and able to damp vibrations, limiting excessive thermal gradients. The second category refers to those technologies that continuously predict and compensate the positioning error throughout the application of suitable sensors and models of the MT structure, implemented into the machine center software.

This works presents a novel active approach that focuses on this second category. The approach consists of developing a new class of "smart adaptronic structures" based on the integration of passive materials, Carbon Fibre Reinforced Polymers (CFRP), with sensing materials (smart sensors) able to measure the deformed conditions of the structure in real-time and to calculate the transposition at the end-effector through an appropriate thermo-mechanical model.

The proposed solution is based on the use of a multiplexed optical fiber sensor with a sufficient number of Bragg gratings for strains measuring (in specific reticular grid points) embedded in the structure. The high sensitivity of the sensors (~ 0.2 με) suggests to employ them in the MT with high stiff structures. These smart sensors (FBG) are suitable to measure both strains and temperature with very high accuracy and resolution [22]. Then, the measurements (linear elongations) obtained by these sensors are post-processed to predict the distortion/deformation of the structure (at tool tip location) in the 3D space domain using special algorithms based on Multiple-Regression Method [23].

2. Concept and Kinematic model formulation

The proposed system is the first phase of an innovative concept to compensate dynamic variations in machine tools. This configuration does not measure the origins of deformations (temperature, load and accelerations) but it determines the distortions of the MT structures and compensate them using a proper robust model.

2.1 Working Principle

In order to extrapolate deviations and calibrate the MT, a set of Fiber-optic Bragg Gratings strain sensors (FBG) is embedded in the vertical axis [24]. FBG sensors may offer many advantages

since they ensure a dynamic performance up to 260 Hz [24], permitting the exposure and measurement of distortions acting during the working operations. The determination of the tool tip displacement is a complex process if it is directly extrapolated from the strains. For this reason, it is more convenient to employ FBG as a displacement sensor and to measure the overall elongation (integral effect) of some critical point-to-point dimensions of the MT geometry.

The proposed adaptive structure consists of an innovative machine tool vertical axis made of CFRP material, which integrates a set of the Fibre Bragg Grating (FBG) displacement sensors (S1-S5), as shown in Figure 1. The FBG sensors have been placed in the vertical-axis structure in order to measure the total axial elongation of each side of the structure in the direction of the fibers orientation, combining static loads and thermal gradients. These on-line measures are used as input in a structural mathematical model that predicts the deviation of the tool tip in three spatial directions. The outcome is an algorithm, represented by linear equations, that is integrated into the computer numerical control (CNC) to compensate the position of the tool tip in real-time during the working operations. The coefficients of the prediction models were calculated using a Multiple Regression Analysis (MRA). The model was built by simulation of the Finite Element Analysis (FEA) applied to the ram that was subjected to different static loads and thermal conditions.

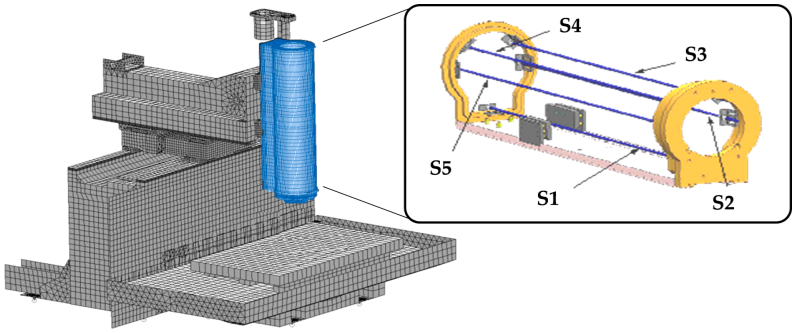

Figure 1. The adaptive structure concept and the sensor locations (internal view).

The working conditions have been simulated through a set of loads representing the undesired factors during the machining. Finally, the model has been validated through a set of experimental tests on a prototype in order to prove the effectiveness of the FBG sensors.

2.2 The embedded distributed sensors

Accurate and reliable measurements of the key variables play an important role to compensate the deviations and to calibrate the MT. The information obtained by these variables are considered for model validation and MT calibration. The temperature sensors are used as inputs to estimate thermal deformations [25-26]. The spindle speed, the axis feed-rate, the machining time and other constants may be the main cause of heat sources.

A traditional approach is based on the temperature distribution evaluation using thermocouples or resistance thermometers [27,28]. This method may show a set of limits, in fact when the number of thermocouples increases on the MT surface, many potential undesired effects may be noted (e.g. electrical disturbs) reducing the effectiveness of the calibration method. On the other hand, a limited number of sensor application does not permit to map correctly the temperature behaviour. Nowadays, infrared technologies may be an effective option to measure the thermal gradient on the surfaces of the MT frames [29,30]. In fact, these systems are able to provide robust measurements of temperature. Nevertheless, they lose information when the calibration system is switched off, compromising the compensation over time.

The FBG strain sensors are able to overpass all these limits, in fact they guarantee robust and permanent measurements and they may be installed in multiple positions embedded in the MT, mapping potential thermal gradients completely. In addition, the FBG sensors have the capacity to detect all potential deviations on the tool tip point (TTP), not only originated by temperature

variability but also when other external factors (e.g. cutting effects) are present. In fact, they may measure directly all point to point deviations of the MT structure surfaces [31].

In particular, FBGs are usually insensitive to magnetic and electric inputs. Certain types of optical fibres have high sensitivity on specific wavelength. Their photo-sensitivity can lead to a variation of refractive when the fibres are open to a specific wave-length (UV range). Other advantages of FBG sensor application are represented by their lightweight, small size, electromagnetic protection, distance conduction and electric inaccessibility [31,32]. These characteristics are particular suitable in manufacturing conditions. In addition, this technology shows multiplexing capabilities providing an absolute measure of strain at multiple points simultaneously [33, 34].

The state of art shows a broad range of FBG applications. They are used to detect damages, to monitor structure health, to control stresses in airplanes and rotor blades of wind turbines or to measure strain in harsh environments [35]. By using these sensors, the modelling process can become simpler, more robust and efficient since the number of sensors can be limited and the effects of thermal hysteresis minimized. Zhou et al. [36] used FBG to investigate the effect of temperature variations of a machine tool on the shop floor. The FBGs work as an optical filter by selecting a certain portion of the input spectrum of the light to be reflected. They are integrated as sensors in optical fibres. When the part of the FBG sensor is deformed due to external disturbances (e.g. strain or temperature), a change in the grating periods is noted modifying the Bragg wavelength. By measuring the wavelength change, the physical quantities can be measured and the temperature effects should be compensated using a proper calibration system. In this way, a FBG sensor is based on the alterations in the reflective signal, which depends on the core and the periodicity of the grating.

The Bragg wavelength is defined as [36]:

$$\lambda = 2 \cdot n_{eff} \cdot \Delta ; \tag{1}$$

where n_{eff} and Δ are the refractive value of the material and the grating structure, respectively. As defined, under temperature or stress influence, the grating dimension changes. The Bragg length shift of $\Delta\lambda$ is modulated by axial deformation change $\Delta\varepsilon$ and temperature range ΔT in the form:

$$\frac{\Delta\lambda}{\lambda} = \left(\alpha_f + \xi\right) \cdot \Delta T + \left(1 - p_e\right) \cdot \Delta\varepsilon ; \tag{2}$$

where λ is the FBG wavelength, p_e, α_f are the photoelastic coefficient and the thermal-expansion value, respectively. The relationship between the temperature fluctuation and the FBG sensor is expressed by the following equation:

$$\Delta\lambda = \left(\alpha_f + \xi\right) \cdot \lambda \cdot \Delta T ; \tag{3}$$

By using the equations (2) and (3) the temperature effect to be compensated may be extrapolated.

2.3 Kinematic linear n-sensor model

Considering a CFRP structure (e.g. a beam) connected by n ideal bars and subjected to a plane in-deformation, and assuming that the maximum allowable displacement range is smaller than 1μm, the movement δL of 2 connected sections can be expressed as:

$$\delta L = L_i - L_{i,0} , \tag{4}$$

where D_i represents the instantaneous length of the i-th bar and $D_{i,0}$ is the distance of the i-th segment, respectively. The relationship between distortions and FBGs movements can be modeled

Peer-reviewed version available at Appl. Sci. 2017, 7, 114; doi:10.3390/app7020114

as shown in figure 2. The actual end effector position includes the effect of kinematic errors, achieved by the composition of three roto-translations. These matrices are defined by the equations (5-9).

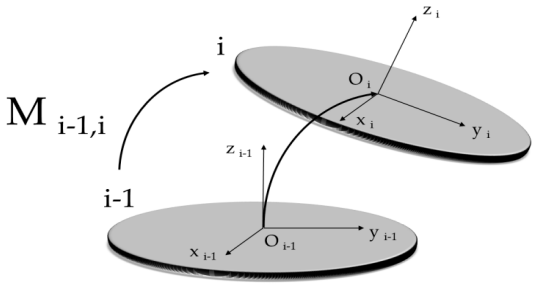

Figure 2. Description of general limited DOF parallel manipulator system.

$$M_{i-1,i} = M^{a}{}_{i-1,i} \cdot M^{b}{}_{i-1,i} \cdot M^{c}{}_{i-1,i}\,, \tag{5}$$

$$M^{a}{}_{i-1,i} = \begin{bmatrix} 1 & 0 & 0 & a \\ 0 & \cos(\alpha_i) & -\sin(\alpha_i) & 0 \\ 0 & \sin(\alpha_i) & \cos(\alpha_i) & 0 \\ 0 & 0 & 0 & 1 \end{bmatrix}, \tag{6}$$

$$M^{b}{}_{i-1,i} = \begin{bmatrix} \cos(\beta_i) & 0 & \sin(\beta_i) & 0 \\ 0 & 1 & 0 & b \\ -\sin(\beta_i) & 0 & \cos(\beta_i) & 0 \\ 0 & 0 & 0 & 1 \end{bmatrix}, \tag{7}$$

$$M^{c}{}_{i-1,i} = \begin{bmatrix} 1 & 0 & 0 & 0 \\ 0 & 1 & 0 & 0 \\ 0 & 0 & 1 & c \\ 0 & 0 & 0 & 1 \end{bmatrix}, \tag{8}$$

where matrices M^a, M^b, M^c elements are exhaustively described in [37, 38]. By considering a vertical slide as a series of elementary parallel manipulator systems, as shown in figure 3, it is possible to generalize the kinematic model for micro-deformation measurements.

In particular, the error calibration and the compensation system of MT can be represented by the equation (9).

$$M_{0,n} = \prod_{i=1}^{n} M_{i-1,i}\,, \tag{9}$$

where the matrices represent the three subsequent functions to transfer the tool tip point of MT from the position (0; 0; 0) to the position (x; y; z). The tool tip point (TTP) is one of the most interesting point in a MT, in fact it represents the ideal contact point between the tool and the workpiece. Any undesired displacements at TTP may generate the machining errors.

A calibration model has been developed to compensate the thermal effects. The nominal TTP position (x; y; z) can be appropriately stated using the transformation matrix formalism as follows:

Peer-reviewed version available at Appl. Sci. 2017, 7, 114; doi:10.3390/app7020114

$$D = i \cdot D_x + j \cdot D_y + k \cdot D_z , \tag{10}$$

where the error spatial components are expressed by equations (11).

$$\begin{aligned} D_x &= \alpha_0 + \alpha_1 \cdot \delta L_1 + \alpha_2 \cdot \delta L_2 + \alpha_3 \cdot \delta L_3 + \alpha_4 \cdot \delta L_4 + \alpha_5 \cdot \delta L_5 \\ D_y &= \beta_0 + \beta_1 \cdot \delta L_1 + \beta_2 \cdot \delta L_2 + \beta_3 \cdot \delta L_3 + \beta_4 \cdot \delta L_4 + \beta_5 \cdot \delta L_5 , \\ D_z &= \gamma_0 + \gamma_1 \cdot \delta L_1 + \gamma_2 \cdot \delta L_2 + \gamma_3 \cdot \delta L_3 + \gamma_4 \cdot \delta L_4 + \gamma_5 \cdot \delta L_5 \end{aligned} \tag{11}$$

δL_j is the elongation measured by the sensor j (j = 1... 5). These errors can depend on the position of the vertical axis along the Z-direction.

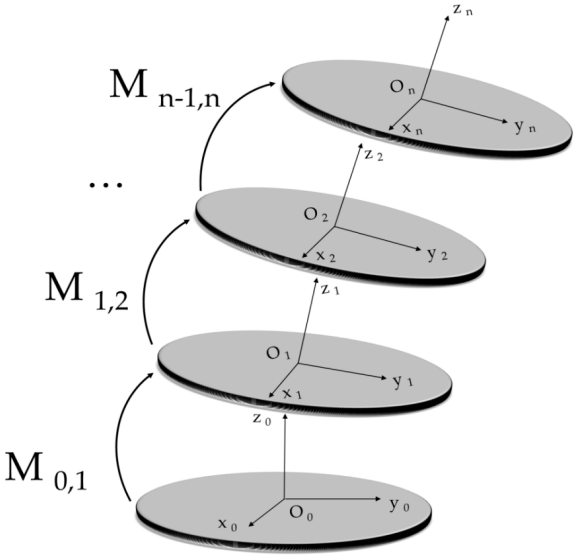

Figure 3. HTM system composition of subsequent reference plane.

In order to investigate the feasibility of the FBG sensor implementation, the first phase was to study the machine tool behaviour through a set of simulations. A model may be built by a Finite Element (FE) analysis that represents the main MT features, focusing on structural parts and sensor positions. The study was performed on a ram of a milling machine and the simulation results are shown in figure 4. The simulation wanted to evaluate if the FBG resolution was able to detect distortions. In particular, the FE study has been performed simulating a set of external generalized loads that may usually occur during the working operations. Figure 4 illustrates the results (strain-tensor) obtained from the FE analysis applying a static force on Y axis. The simulation has been used to estimate the coefficients of the regression equations.

In the same way, the FE analysis has been replicated considering the thermal stresses. The objective was to simulate and measure the displacements in different parts of the structure where the FBG sensors were located. By using this information a further adjustment of the regression model has been executed in order to predict the TTP position accurately.

Peer-reviewed version available at Appl. Sci. 2017, 7, 114; doi:10.3390/app7020114

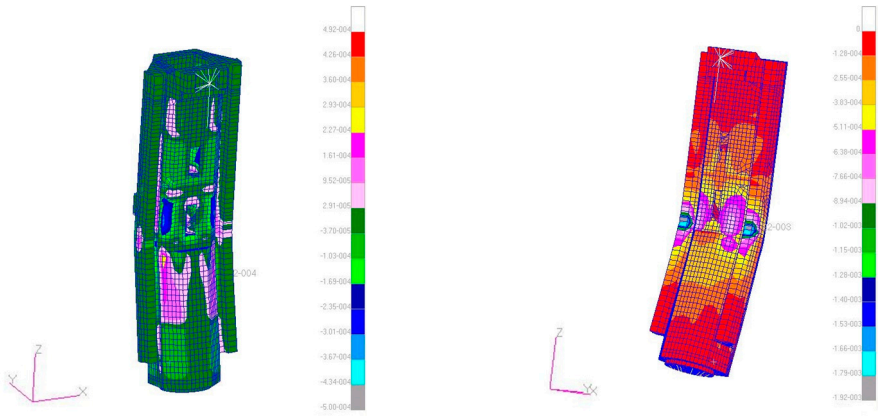

Figure 4. A set of overviews of the FE analysis results (strain-tensors) performed on the CFRP beam with the embedded FBG sensors applying a static load on Y axis.

2.4 Test-bench setup validation and procedure

In the light of the obtained results from numerical simulations, a prototype (a milling machine ram) has been fabricated and tested. The scope was to compare the numerical models with the experimental tests using the FBG sensors.

Figure 5 shows an overview of the calibration system prepared to perform the experimental tests. The test-bench was composed by the moving slide frame with the embedded FBG sensors, the interrogator and a PC to process the collected data. The axis structure has been constrained in X-Y directions at the carriages location and in Z direction at the nut support location.

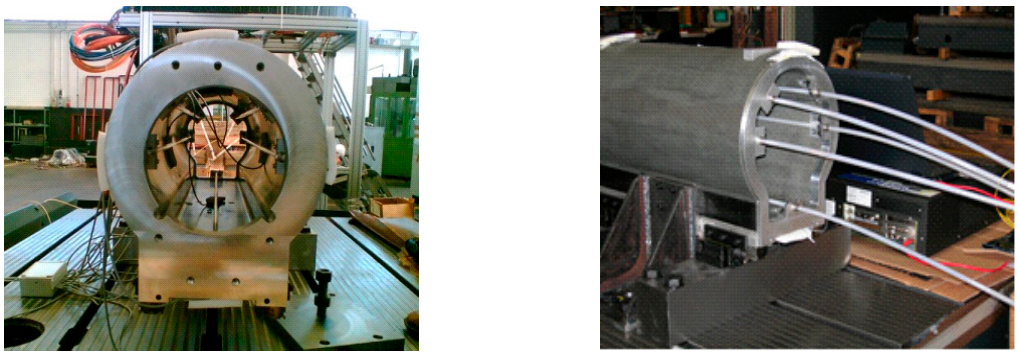

(a) (b)

Figure 5. Test-bench setup of the prototype with the embedded FBG sensors.

The experimental procedure consisted in two main phases. In the first part of the test campaign, a set of static loads has been applied to the structure in order to verify the effectiveness of the FBG sensors embedded in the prototype. These results have been compared with the numerical model.

The stresses measured by the FBG sensors through the modification of their characteristics were transferred to a PC. The signals were examined and saved by the sensing software. The obtained results have permitted to improve the regression model to compensate the TTP deviation.

The second phase of the experiments was based on the time-variant thermal tests. In this case, the experimental tests have been performed varying the temperature of the structure over time (36 hours). This part of the study wanted to optimize the model and understand the effectiveness of the calibration system in compensating the TTP position when the MT structure temperature varies.

The measures of the FBG sensors have been acquired by an optical reading unit (Fabry-Perot Interferometer), while the temperature changes of the MT ram have been automatically collected by an integrated circuit temperature sensors (LM35) located along the structure. The tool tip drift has been detected through a displacement sensor based on a laser interferometer.

3. Experimental tests and results

The compensation of thermal-mechanical errors is based on an effective kinematic model able to represent the potential point to point deviations due to external generalized loads (in this case, mainly temperature). Usually, the thermal strains are a supplementary component that is summed to the geometrical errors when there is a variation of the structure temperature gradient. For this reason, the mathematical model needs to be expressed as follows:

$$f\left(\Delta T_1, \Delta T_2, ..., \Delta T_n\right) = A_1' \cdot \Delta T + \Delta T' \cdot A_2 \cdot \Delta T \,, \tag{12}$$

where A_1 is the coefficient vector and A_2 is the matrix of the regression model, while ΔT represents the temperature intensification vector of the frame. In order to tune the model, a stepwise regression with a programmed exploration algorithm has been applied. This technique is able to categorize linear formulations at each stage counting or removing a factor using ANOVA or other techniques. The experimental campaign has considered the results of a set of tests performed in static and dynamic conditions. In the first case, the model has been validated applying a static load to TTP, while in the second part of the research the model has been evaluated while the thermal conditions varied. In both cases, the model has been analyzed comparing the predicted deviations with real measurements of the TTP positions.

3.1. The static experimental tests for model validation

The first campaign of experimental test has been performed applying a set of static loads to the tool tip points. These tests aimed at verifying the model obtained by the numerical analysis. In particular, by using the experimental results it was possible to improve the estimation of the equation coefficients to calibrate the system.

Figure 6 shows the displacements (μm) measured by the FBG sensors when a set of static forces (1,000-2,000-3,000-4,000N) have been applied to the tool tip. In particular, figure 6(b) illustrates the variability of the displacements detected by the sensors that were located in different positions on the ram surface. This variability highlights the relationship between the sensor positions and the magnitude of the applied loads.

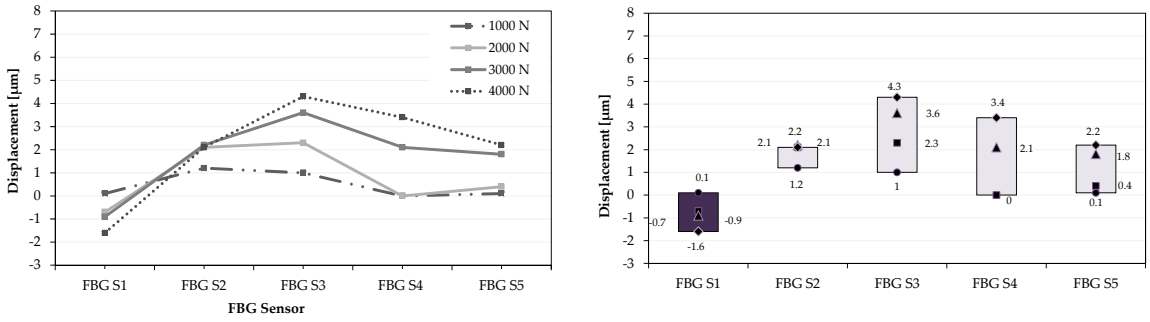

Figure 6. The displacements (μm) measured by the FBG sensors applying a set of static forces.

The position of each FBG sensor is critical to detect the stress measured on the MT frame. As defined, an increase of the sensor number has not significant impact on the material isotropy.

The first validation campaign has been conducted applying a set of static forces at TTP and comparing the real tip displacement measured by an interferometer with the predicted position defined by the model prediction equations, as shown by equations 10-11. Figure 7 presents the comparison between the real and the predicted displacement (Y direction) of the tool tip point by varying the static load.

Peer-reviewed version available at Appl. Sci. 2017, 7, 114; doi:10.3390/app7020114

The obtained results show a substantial matching between the real and predicted positions. In particular, the model has an acceptable accuracy that is close to 5% in the load range (1,000-4,000N).

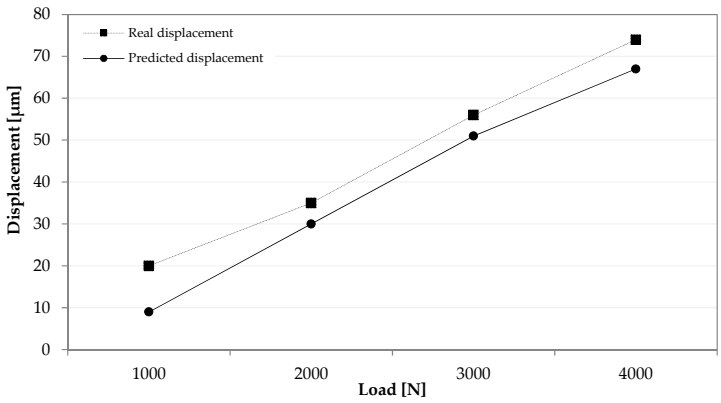

Figure 7. The static force effects: a comparison between the real tool tip displacement and the predicted position when a static force is applied to the tool tip point.

3.2. The time-variant experimental tests for model validation

In the second part of the experimental campaign, a set of time-variant experiments has been executed. In particular, the prototype was subjected to the application of thermal loads over a prescribed time period of 36 hours. By starting with an environmental temperature close to 30°C, the frame conditions have been monitored measuring the thermal stresses in the different positions of the frame surface. A preliminary investigation permitted to improve the regression coefficients extrapolated from the FE study in order to obtain a robust model of the thermal effects. In this way, a multivariate regression model was studied to fit the Z-axis thermo-mechanical deformations.

Figure 8 presents the displacement variability detected by the sensors during the experiment time. The temperature of the structure was automatically collected by integrated circuit temperature sensors (LM53) located along the ram.

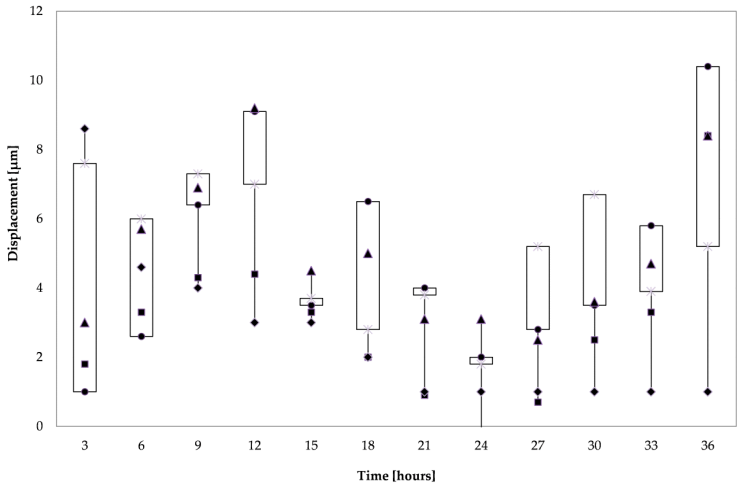

Figure 8. Variations measured by FBG sensors arranged over 36 hours experimental tests.

By using the experimental data, a Multi Regression Analysis has been performed, estimating . the thermal-mechanical model coefficients. In addition, further temperatures of strategical positions (ΔTbulk, ΔTsurf and ΔTflange) have been collected by a set of thermocouples and included in the model as independent variables.

Equation 13 represents the mathematical formulation of MRA technique.

Preprints (www.preprints.org) | NOT PEER-REVIEWED | Posted: 29 December 2016 doi:10.20944/preprints201612.0139.v1

Peer-reviewed version available at Appl. Sci. 2017, 7, 114; doi:10.3390/app7020114

$$\Delta Y_{pred} = \alpha_0 + \alpha_1 \cdot \Delta S_1 + \alpha_2 \cdot \Delta S_2 + \alpha_3 \cdot \Delta S_3 + \alpha_4 \cdot \Delta S_4 + \alpha_5 \cdot \Delta S_5 + + \alpha_6 \cdot \Delta T_{bulk} + \alpha_7 \cdot \Delta T_{surf} + + \alpha_8 \cdot \Delta T_{flange} \quad , \qquad (13)$$

where ΔT_{bulk} is the variation of Z-axis bulk temperature between the starting time and the instant of measure, ΔT_{surf} is the difference between bulk RAM temperature and Surface temperature, and ΔT_{flange} is the temperature range measured between the spindle case and the structure. Table 1 summarizes the results of the MRA model with the use of a stepwise software.

Table 1. Multiple Regression Equation coefficients.

Coefficients	Description	Value	Standard Error
α_0	Intercept	-0.002	0.005
α_1	FBG Sensor 1	10.097	2.552
α_2	FBG Sensor 2	1.836	4.626
α_3	FBG Sensor 3	-10.063	4.575
α_4	FBG Sensor 4	0.678	5.896
α_5	FBG Sensor 5	-5.138	6.137
α_6	Delta T bulk	0.002	0.020
α_7	Delta T surface	-0.028	0.022
α_8	Delta T flange	0.010	0.013

Figure 9 presents the thermal study results. A substantial coherence between the real and predicted position of the tool tip point is noted over time (36h). The curves have the same change trends. The MRA models is able to fit the thermos-mechanical deformations with some mismatching due to the limited number of sensors integrated into the structure. The obtained accuracy of the predicted model varies from 5% to 8%, guaranteeing a substantial effectiveness of the model to predict the tool tip deviations. In the proposed experiments, the temperature effects had an important influence on the TTP position, in fact the maximum detected deviation was equal to 51 micron. If compensation is not provided, the total error due to the thermo-mechanical effects is described by the dotted curve in figure 9. By using the predicted model the TTP position may be corrected. The potential compensation is equal to the difference between the dotted line and the solid line in figure 9. In this case, the maximum model error is close to 9 micron.

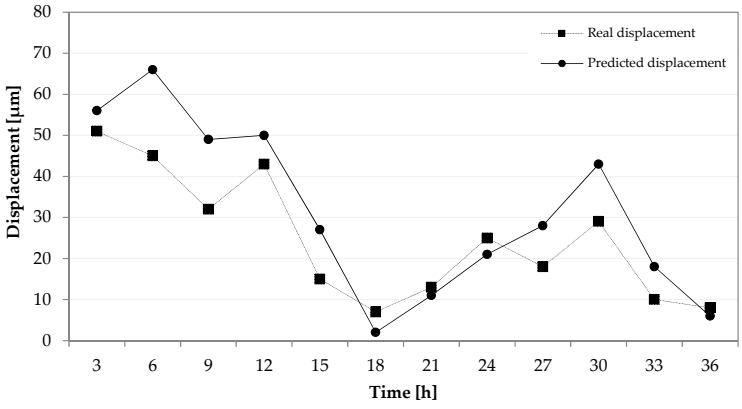

Figure 9. Thermo-mechanical effects: the real tool tip displacement vs. the predicted displacement.

The obtained results underlined the effectiveness of the FBG sensors in detecting the structure stresses due to external loads (e.g. temperature variation). The application of FBG sensors shows many advantages, in particular, they are able to measure stresses from different types of sources (e.g.

Peer-reviewed version available at Appl. Sci. 2017, 7, 114; doi:10.3390/app7020114

load, temperature, accelerations) in real-time. This fact permits to obtain a model that is able to predict the TTP position when any type of stress occurs on the MT structure. On the other hand, the model needs to be optimize in order to reduce the predicted errors increasing the number of sensors and improving the regression technique. Table 2 shows a summary of the main advantages and limits of the FBG sensor application.

Table 2. A comparison between the main advantages and limits of the FBG sensor application.

Advantages	Limits
– high sensitivity (0.2 μ = 0.2μm/m = 0.00002% in strain; 0.5 °C in temperature); – maximum strain 1%; – small size (diameter ~ 0.5 mm) and light weight; – immunity to electromagnetic interference; – immunity to chemical agents; – geometrical versatile; – temperature range -40 °C 300 °C; – ability to be embedded or laminated into structures; – high durability and lifetime over 20 years.	– due to their high sensitivity, the measurement of one quantity (e.g. strain) may be influenced by the other quantity; – fibers cannot be repaired; – complexity in fibers handling due to their brittleness; – relatively high costs, but they depend on the type of application; – not always ease of installation to obtain an effective application – complexity in statistical data management to identify a robust model;

4. Conclusion

This study aims to present a structured method to calibrate a MT when it is affected to undesired external factors. The MT calibration is a critical process since it permits to compensate geometrical or thermal errors instantaneously, guaranteeing the machining performance. The conventional approaches are based on models able to predict the MT deformations, studying a relationship between machine accuracy and undesired loads. Nevertheless, it is difficult to identify a general robust relation and these models need to be calibrated for every machine variant limiting their success, increasing costs and the implementation time.

The proposed solution is based of a novel approach to calibrate a machine tool in real-time, analyzing the thermo-mechanical errors through Fibre Bragg Grating (FBG) sensors embedded in the MT frame. This configuration consists of an adaptronic structure of passive materials, Carbon Fibre Reinforced Polymers (CFRP), equipped by FBG sensors that are able to measure in real-time the deformed conditions of the frame. By using a proper thermo-mechanical kinematic model, the displacement of the end effector may be predicted and corrected when it is required. By starting from a set of FE simulations, a relationship between the FBG behaviors and TTP displacement was evaluated. The simulations were performed varying a static load at TTP and the structure temperature. The multiple regression permitted to identify a model to be validated through a set experimental tests. A prototype (a ram of a commercial milling machine) was fabricated integrating the FBG sensors in the MT frame. In the first part of the experimental tests, the model was validated applying a set of static loads. This analysis showed a good matching between the real and the predicted position of the MT tool tip point. In the same way, the tests were replicated varying the environmental temperature over time (36h). These results obtained by the FBG measures allowed to tune the regression model and to improve the error prediction. The last campaign of experimental tests illustrates a substantial coherence between the real and predicted position of TTP. This study highlights the significant advantages to apply FBG sensors in MT calibration such as their high sensitivity, geometrical versatility, light weight, immunity to electromagnetic interference or chemical agents, high durability. Nevertheless, it also underlines the limits of this method. In particular, the accuracy of the model depends on the number and the position configuration of the sensors implemented in the structure. The choice of specific statistical methods may improve the accuracy of the model. In the light of these results, the next steps of the research will be based on the

fabrication of new prototypes changing the position configuration of the FBG sensors. The collected data will be analyzed by further techniques to reduce the model error.

References

1. Altintas, Y.; Manufacturing automation. *Cambridge: Cambridge university press*, **2000**.
2. Pahk, H.J.; Thermal error measurement and real time compensation system for the CNC machine tools incorporating the spindle thermal error and the feed axis thermal error. *Adv Manuf Tech*, **2002**, 20, pp. 487–94.
3. Li, J. W.; Zhang, W. J.; Yang, G. S.; Tu, S. D.; Chen, X. B.; Thermal-error modeling for complex physical systems: The state of arts review. *International Journal of Advanced Manufacturing Technology*, **2009,** 42, 1-2, pp. 168-179.
4. Ramesh, R.; Mannan, M.; Poo, A.; Error compensation in machine tools—a review: part I: geometric, cutting-force induced and fixture-dependent errors, *Int J Mach Tools Manuf* , **2000**, 40, pp. 1235–1256.
5. Biral, F.; Bosetti, P; On-line measurement and compensation of geometrical errors for Cartesian numerical control machines. *AdvancedMotion Control '06*, **2006**, volume 1, Advanced Motion Control, IEEE, Istanbul, pp. 120–125
6. Degarmo, E. P.; Black, J. T.; Kohser, R. A.; Materials and Processes in Manufacturing, *9th ed. John Wiley &* Sons, **2003**.
7. Fung, E. H.; Yang, S. M.; An approach to on machine motion error measurement of a linear slide, *Measurement*, **2001**, volume 29, no. 1, pp. 51–62.
8. Choi, J.; Min, B.; Lee, S.; Reduction of machining errors of a three-axis machine tool by on-machine measurement and error compensation system, *Journal of Materials Processing Technology,* **2004**, volume 155-156, pp. 2056–2064.
9. Song, Y. W.; Starodubov, D.; Pan, Z.; *IEEE Photonics Technology Letters 14*, **2002**, pp. 1193.
10. Mayr, J.; Jedrzejewski, J.; Uhlmann, E.; Thermal issues in machine tools, *CIRP Ann. Manuf. Tech.*, **2012**; 61, pp. 771–91.
11. Aggogeri, F.; Borboni, A.; Faglia, R.; Merlo, A.; De Cristofaro, S.; Precision Positioning Systems: An overview of the state of art, *Applied Mechanics and Materials,* **2013**, 336-338, 1170-1173.
12. Ramesh, R.; Mannan, M.; Poo, A.; Error compensation in machine tools – a review: Part II: thermal errors, *International Journal of Machine Tools Manufacture*, **2000**, n. 40, pp. 1257–1284.
13. Mian, N.S.; Fletcher, S.; Longstaff, A.P.; Myers, A.; Efficient estimation by FEA of machine tool distortion due to environmental temperature perturbations, *Precis. Eng.*, **2013**, 37, pp. 372–9.
14. Bossmanns, B.; Tu, J.F.; A thermal model for high speed motorized spindles, *Int JMach Tools Manuf,* **1999**, 39, pp. 1345–66.
15. Chen, J.; Yuan, J.; Ni, J.; Thermal error modelling for real-time error compensation, *Int J Adv Manuf Techno.,l* **1996,** 12, pp. 266–75.
16. Pellegrini, N.; A thermo-dynamical constitutive model based on kinetic approach for shape memory materials, *Advanced Materials Research,* **2013**, 651, pp. 42-48.
17. Chen, J.; Chiou, G.; Quick testing and modeling of thermally-induced errors of CNC machine tools, *Int J Mach Tools Manuf.*, **1995**; 35, pp. 1063–74.

18. Lee, J.H.; Yang, S.H.; Development of thermal error model with minimum number of variables using fuzzy logic strategy, *KSME Int J*, **2001**, 15, pp. 1482–9.
19. Abdulshahed, A.; Longstaff, A.P.; Fletcher, S.; Myers, A.; Comparative study of ANN and ANFIS prediction models for thermal error compensation on CNC machine tools, *Laser metrology and machine performance,* **2013**, pp. 79–88.
20. Wang, K.C.; Thermal error modeling of a machining center using grey system theory and adaptive network-based fuzzy inference system, *Cybernetics and intelligent systems,* **2006**, pp. 1–6.
21. Wang, Y.; Zhang, G.; Moon, K.S.; Sutherland, J.W.; Compensation for the thermal error of a multi-axis machining center, *J Mater Process Technol*, **1998**, 75, pp. 45–53.
22. Wang, K.C.; Thermal error modeling of a machining center using grey system theory and HGA-trained neural network, *Cybernetics and intelligent systems*, **2006**, pp. 1–7.
23. Teti, R.; Jemielniak, K.; O'Donnell, G.; Dornfeid, D.; Advanced monitoring of machining operations, *CIRP Ann-Manuf Technol*, **2010**, 59(2), pp. 717–39.
24. Franco-Gasca, L.A.; Herrera-Ruiz, G.; Vera, R.P.; Troncoso, R.J.R.; Leal-Tafolla, W.; Sensorless tool failure monitoring system for drilling machines. *Int J Mach Tools Manuf*, **2006**, 46(3), pp. 381–6.
25. Walter, M.M.; Norlund, B.; Koning, R.J.; Roblee, J.W.; Error budget as a design tool for ultra-precision diamond turning machines. *Proceedings of the ASPE's 17thAnnual Meeting,* **2002**.
26. Chen, C.; Zhang, J.F.; Wu, Z.J.; Feng, P.F.; Real-time measurement of machine tool temperature fields and their effect on machining errors. *Mechanika*, **2011**, 17(4), pp. 413–7.
27. Law, M.; Rentzsch, H.; Ihlenfeldt, S.; Evaluating mobile machine tool dynamics by substructure analysis. *Adv Mater Res*, **2014**, 1018, pp. 373–80,
28. Xie, C.; Roddeck, W.; Liu, C.S.; Zhang, W.M.; The analysis and research about temperature and thermal error measurement technology of CNC machine tool. *Manuf Autom Tech*, **2009**, pp. 40–4.
29. Heisel, U.; Thermography-based investigation into thermally induced positioning errors of feed drives by example of a ball screw. *Ann CIRP*, **2006**, 55(1), pp. 423–6.
30. Mayrl, J.; Comparing the thermo-mechanical behaviour of machine tool frame designs using a FDM-FEM simulation approach. *Proceedings of the ASPE Annual Meeting,* **2007**, pp. 17–20.
31. Mihailov, S.J.; Fiber Bragg grating sensors for harsh environments. *Sensors,* **2012**, 12, pp. 1898–918.
32. Zhang, R.; Zheng, S.; Xia, Y.; Strain profile reconstruction of fiber bragg grating with gradient using chaos genetic algorithm and modified transfer matrix formulation. *Opt Commun*, **2008**, 281(13), pp. 3476–3485.
33. Guo, H.L.; Xiao, G.Z.; Mrad, N.; Yao, J.P.; Fiber optic sensors for structural health monitoring of air platforms. *Sensor,* **2011**, 11, pp. 3687–705.
34. James, S.; Dockney, M.; Tatam, R.; Simultaneous independent temperature and strain measurement using in-fibre bragg grating sensors. *Electron Lett*, **1996**, 32(12), pp. 1133–1134.
35. Ren, L.; Jia, Z.G.; Li, H.N.; Design and experimental study on FBG hoop-strain sensor in pipeline monitoring. *Opt Fiber Tech,* **2014**, 20, pp. 15–23.

36. Zhou, Z.; Liu, W.Q.; Huang, Y.; Wang, H.P.; He, J.P.; Huang, M.H.; Optical fiber Bragg grating sensor assembly for 3D strain monitoring and its case study in highway pavement. *Mech Syst Signal Pr*, **2012**, 2, pp. 36–49.
37. Legnani, G.; Casolo, F.; Righettini, P.; Zappa, B.; A homogeneous matrix approach to 3D kinematics and dynamics - I. Theory. *Mechanism and Machine Theory*, **1996**, 31, 5, pp. 573-587.
38. Xia, H.; Byrd, D.; Dekate, S.; Lee, B.; High-density fiber optical sensor and instrumentation for gas turbine operation condition monitoring. *Journal of Sensors*, **2013**, 20, pp. 673-8.